

New Light on Salt Eutectic Structures - use of the Raman Microscope

Rolf W. Berg and David H. Kerridge

Department of Chemistry, DTU Building 207, Technical University of Denmark
Kemitorvet, DK-2800 Lyngby, Denmark

Key words: Raman, microscopy, conglomerate, melt, solid, structure, nitrate, nitrite, imaging

Submitted on July, 24, 2000.

E-mail: rwb@kemi.dtu.dk. <http://struktur.kemi.dtu.dk/raman/raman.html>

ABSTRACT

This paper presents the first computer mappings, resulting from the use of the Raman microscope, of the structures of salt eutectics solidified from their melts.

The distribution of the components of the six salt eutectics examined (five binary and one ternary system) showed considerable general similarity, in that the components were concentrated into roughly rounded areas of about 0.5 to 5 μm across, the areas alternating in both directions across the sections. These structures are best described by the term "*conglomerate*". The areas did not consist of the pure components, though they had high concentrations of one component and probably represented the limiting solid solutions into which the molten eutectics separated on solidification. These "*conglomerate*" structures are very different from those of metallic eutectics which are well known frequently to form lamellar arrangements of the component phases and it had been expected that these latter would also be found generally in salt eutectics.

Changes in composition, in sectioning direction and in solidification technique were found to result in relatively small differences. The major effect was found to result from the rate of solidification, faster cooling causing markedly smaller rounded areas with the "*conglomerate*" becoming much finer grained.

In every case there was very considerably more interfacial contact between the solid solutions than would have been expected by analogy with the crystallites of the single pure component salts. This high "interphasial" area of contact is considered to result in the unexpectedly high electrical conductivity of solid salt eutectics previously found. In addition these large interphasial areas would give rise to the recently discovered enthalpy term, which together with the enthalpies of solid solution formation, produce the melting enthalpy differences between those of solidified salt eutectics and those of the corresponding unmelted mechanical mixtures of the components.

INTRODUCTION

The study of the structure of solid salt eutectics has not commanded much attention hitherto, despite the fact that the chemistry of molten salt eutectics has been the object of a large volume of research.

It is common knowledge that the binary eutectic composition separates on freezing into two solid phases, based on the two components A and B, but since solid solutions are often formed the phases are designated α and β (α being a solution of B in A, etc.). However the spatial arrangement(s) that the two phases take up in the solid is almost wholly unknown and has been unquestioned by the majority of chemists. Similarly with ternary and higher eutectics.

In contrast metallurgists have devoted great efforts to understanding the structures of metallic eutectics and have frequently reported rapidly alternating phases of lamellar or fibrous forms.

Only two groups of workers appear to have published studies on solid salt structures; their photomicrographs show largely lamellar structures for LiF/NaF though one showed a fibrous structure [1,2] and consistently fibrous structures for NaF/NaCl [1,2]. More recent work has shown lamellar structures for LiF/LnF₃ (where Ln = La or Pr), fibrous for LiF/GdF₃ or a mixture of the two (for Ln = Nd or Sm) [3,4]. A lamellar structure was claimed for PbF₂/ScF₃ [5].

From this list it is evident that the systems chosen for publication have been somewhat restricted and that it would be of considerable interest to examine a wider range of compounds and desirably some non-fluoride systems. This is particularly relevant because measurements [6,7] on the electrical conductivity of solid salt eutectics have shown these to be two or more orders of magnitude higher than would be expected by extrapolation from the electrical conductivities of the component single salts. In contrast the electrical conductivities of the molten eutectics were in the range expected from extrapolation of the values for the molten single salts. This difference has been attributed to the large area of interfacial contact between the phases α and β , and significantly, was found with a wide range of binary and ternary eutectics of oxyanions, halides and even for organic-salt systems. Furthermore this feature was not particularly dependent on the nature of the solidification process (rate and direction of cooling, etc.) [6,7].

More recently evidence has emerged that the melting enthalpy of solid eutectics includes a component due to the large area of contact between the solid phases α and β [8,9]. Once more this large "interphasial" area was found for all the eutectics so far examined and again this was not strongly dependent on the solidification conditions.

The Raman microscope is particularly well adapted to identify the eutectic structures formed with oxyanion compounds, since such anions often have quite different Raman active vibrational modes with different frequencies and conveniently high intensities. Thus a number of relatively low melting eutectics, mainly of nitrates and nitrites have been prepared by various cooling regimes, sectioned, ground and polished and examined by Raman microscopy.

The principle of confocal Raman microscopy (mapping) is based on the automatic successive recording of Raman spectra from many points (or pixels)

of a flat sample surface by use of a motorized microscope table, and from these spectra a Raman mapping is computed, based on band intensities at specific wavelength intervals [10].

The Raman spectra of the investigated ions, NO_2^- , NO_3^- and CrO_4^{2-} are well known [11].

The unperturbed nitrite ion is a non-linear species of C_{2v} symmetry with three fundamentals: $\nu_1(A_1)$, Raman active at $\sim 1330 \text{ cm}^{-1}$, $\nu_2(A_1)$, Raman active at $\sim 810 \text{ cm}^{-1}$, and $\nu_3(B_2)$, Raman active at $\sim 1250 \text{ cm}^{-1}$. The nitrate ion is a triangular planar species of D_{3h} symmetry with four fundamentals: $\nu_1(A'_1)$, Raman active at $\sim 1050\text{-}1070 \text{ cm}^{-1}$, $\nu_2(A''_2)$, only IR active at $\sim 830 \text{ cm}^{-1}$, $\nu_3(E')$, Raman and IR active at $\sim 1380 \text{ cm}^{-1}$, and $\nu_4(E')$, Raman and IR active at $\sim 715 \text{ cm}^{-1}$ [11,12]. The chromate ion is tetrahedral of T_d symmetry with four fundamentals: $\nu_1(A_1)$, Raman active at $\sim 850 \text{ cm}^{-1}$, $\nu_2(E)$, Raman active at $\sim 350 \text{ cm}^{-1}$, $\nu_3(F_2)$, Raman and IR active at $\sim 890 \text{ cm}^{-1}$, and $\nu_4(F_2)$, Raman and IR active at $\sim 380 \text{ cm}^{-1}$. The band positions depend somewhat in the kind of cation and the crystal phase, see e.g. data on nitrates [13-15].

EXPERIMENTAL

The eutectics examined and their melting points are given in the table below:

Eutectic Mixture	Composition	Melting Point
$\text{NaNO}_2 / \text{NaNO}_3$	59 : 41 mol%	227 °C
$\text{KNO}_2 / \text{KNO}_3$	24 : 76 mol%	316 °C
$\text{NaNO}_3 / \text{KNO}_3$	50 : 50 mol%,	220 °C
$\text{KNO}_3 / \text{Ca}(\text{NO}_3)_2$	65.8 : 34.2 mol%,	145 °C
$\text{NaNO}_2 / \text{NaNO}_3 / \text{KNO}_3$	48.9 : 6.9 : 44.2 mol%,	142 °C
$\text{KCl} / \text{K}_2\text{CrO}_4$	25 : 75 mol%,	368 °C

The compounds of "*pro analysi*" quality were dried, weighed out in the specified proportions, ground together and melted in 10 mm inner diameter pyrex tubes drawn out to a point at their lower ends.

Two methods of heating and cooling were usually employed. Firstly in a well insulated furnace electronically controlled to cool at 1° , or at $0.1 \text{ }^\circ\text{C}$ per hour, with in some cases a massive aluminium block wired to the lower end and partly outside the isothermal section so as to provide a thermal gradient. Secondly in a temperature controlled furnace, previously used for zone refining, where the tube was slowly pushed downwards from a heated section at a rate of 5mm/hour. The tubes were of Pyrex of 10 mm inside diameter with rounded ends or with ends drawn to a point. Visual inspection showed the molten eutectics to initially solidify to transparent / translucent solids which turned white and opaque on further cooling possibly due to differential thermal contraction and/or to phase changes.

The solidified eutectics were broken out of their container tubes and ground with paraffin, on a metallurgical polishing machine, in the specified direction

with, successively, P220 and 1200 Carborundum papers and finally with a lap impregnated with 0.25 micron diamond paste. The best results were obtained when lubricating with paraffin, washed off with n-pentane. Other lubricants (ethylene glycol, water) and washing liquids (acetone) were tried but resulted in dissolution of more of the salt surface.

Raman spectra were measured with a DILOR XY CCD spectrometer with both macro and microscope entrances. Spectra were excited with an Ar⁺ ion laser light of about 1W power at 514.5 nm wavelength. The Rayleigh line was filtered off by using a Kaiser holographic SuperNotch-Plus filter (approximately 200cm⁻¹ cut-off). The Raman light was dispersed onto a liquid nitrogen cooled CCD detector by use of a 1800 lines/mm grating in an 800 mm focal length single spectrograph, or in a second spectrograph with a much shorter focal length and a grating with 600 lines/mm. In both cases the slits were set to 100 μm corresponding to a spectral resolution of about 4-5 cm⁻¹. A sheet polaroid analyser, which permitted vertically or horizontally polarised light to pass followed by a quarterwave depolariser, was used to check polarization data. Calibration of wavenumber scales to an accuracy of ±1 cm⁻¹ could be done with neon lines superimposed on the spectra; if not calibration errors as large as 30 cm⁻¹ were often obtained [16]. The spot size was generally 1 μm and a 40x40 matrix of points was normally used. Spectral and image files were collected as ".tsf" and ".tvf" format files with the DILOR Labspec program. The microscope table was controlled by the software. Raman band areas were calculated by the software without the background. Mappings were smoothed from pixel to pixel and an artificial colour scale added to obtain better Raman imaging. Band positions were found with the software without any smoothing, employing mixed gaussian-lorentzian bandshapes and built-in baseline correction procedures. Other details are given in the figure captions or have been given previously [17].

The LINKAM temperature controlled hot-stage (HFS91/TP93) [18] was used to examine some NaNO₂ / NaNO₃ specimens at temperatures up to 300 °C. Small pieces of previously solidified samples were directly placed horizontally on the microscope table which was operated from the computer which also controlled the data acquisition.

RESULTS

The Raman signal strength was found to vary considerably from spot to spot for most samples, because of the sensitivity of the focus adjustment and lack of flatness at high microscope magnification; i. e. the sample was often partly out of focus. Thus, instead of using the absolute signal to compose the mappings, it was found that better images could be obtained by using the ratio of selected bands.

For points out of focus both bands decreased in the same manner but the ratio was invariant though subject to noise.

A typical Raman microscopy result is shown in Fig. 1A for the NaNO₂ / NaNO₃ system. The Raman mapping clearly showed that there was considerable

segregation of the eutectic components, although under the optical microscope polished surfaces for this and other samples were virtually featureless. The same segregation features were seen for other Raman mappings of this and other systems. Here, in Fig. 1A, the chemical components were gathered into rather irregular, roughly circular, masses, of about 0.5 to 5 μm across, with compositions ranging from high in nitrite to high in nitrate, both with smaller concentrations of the other constituent, though without large areas approximating to equimolar mixtures (separate measurements on the solid single salts and their mixtures showed that the Raman intensity scale in Fig. 1A, - because of different Raman scattering efficiencies in nitrate and nitrite - should be divided by a factor, perhaps ~ 1.25 to convert it to concentration ratios).

The roughly circular areas seen in Fig. 1A may perhaps best be described as a "conglomerate" structure (to adapt the geological term), and it should also be noted that A. R. Ubbelohde in his book "The Molten State of Matter" [19] used the word "conglomerate" to describe solid salt eutectics, though without citing any evidence or literature reference.

Some preliminary SEM studies [20,21] suggest the fracture surface of a solid eutectic ($\text{NaNO}_3/\text{KNO}_3$) shows packed roughly spherical masses also measuring up to 5 μm across. The cross sections found in this work could well arise from sectioning randomly through such closely packed irregular sized spherical lumps.

Some specimens were cooled at 0.1 $^\circ\text{C}/\text{min}$ in the LINKAM hot stage attachment which also showed similar but finer "conglomerate" structures. On cooling to about 175 $^\circ\text{C}$ the largely transparent solid became opaque but no significant changes in the Raman spectra were observed. Thus no positive evidence for the phase transition reported by Bergman et al. [22] at that temperature could be obtained by Raman spectroscopy. The loss of transparency could also be attributed to differential thermal contraction.

The same general appearance of a "conglomerate" structure was found for all 38 samples of the six eutectics examined, and no marked variation was seen whether the solid sections were taken parallel to the axis of the container tube, at right angles or at 45 $^\circ$. Generally axial sections, i.e. at 90 $^\circ$ to the tube axis, were used. The most marked variation between specimens depended on their cooling rate, where the faster rates resulted in finer "conglomerates", as can be seen from Fig. 2A (1 $^\circ\text{C}/\text{hour}$) which has smaller areas than Fig. 3A (5 mm/hour). The latter figure shows a structure which was one of the closest approaches to a laminar structure found in this work.

As would be expected the more rapidly cooled samples showing a finer "conglomerate" structure would be expected to have larger interphasial area effects and indeed a reduction in the melting enthalpy difference was found for slowly cooled (0.1 $^\circ\text{C}/\text{hour}$) samples of $\text{NaNO}_2/\text{NaNO}_3$.

The only ternary eutectic examined ($\text{NaNO}_2/\text{NaNO}_3/\text{KNO}_3$) gave similar "conglomerate" mappings (Fig. 4), though here separate $\text{NaNO}_3/\text{KNO}_3$ (Fig. 4A) and $\text{NO}_2^-/\text{NO}_3^-$ (Fig. 4B) ratios were obtained from the same spectra.

Fig. 1. Raman (Fig. 1A) and standard optical microscope mapping (Fig. 1B) of a 59/41 molar ratio sample of $\text{NaNO}_2/\text{NaNO}_3$. This sample was melted and solidified in contact with a heat conducting aluminum tube at a cooling rate of $0.1\text{ }^\circ\text{C/hr}$ in the stationary furnace. The solid was sectioned at 90° to the tube axis, and ground. The Raman mapping was based on 40×40 spectra providing the intensity ratio for the bands seen at $\sim 1329\text{ cm}^{-1}$ (NaNO_2) and $\sim 1068\text{ cm}^{-1}$ (NaNO_3). An enlargement of a section of the mapping is shown in Fig. 1C. Examples of spectra obtained in the dark, blue areas (spectrum in blue colour, mostly NaNO_3) and white areas (spectrum in red colour, mostly NaNO_2), for points at {80.7, 31.7} and {82.5, 34.5}, are given in Fig. 1D. The pixel size and spatial resolution were $1\text{ }\mu\text{m}$, obtained with a 100 X objective, a $180\text{ }\mu\text{m}$ confocal hole, a $100\text{ }\mu\text{m}$ slit width, excited with 200 mW of 514.5 nm of Ar ion laser light. Each pixel was exposed twice for 1 second and averaged, followed by an automatic cosmic-ray spike-removal procedure in the software. Note: The Raman spectral abscissa is not calibrated.

Fig. 2. Raman microscope mapping (Fig. 2A) of a 50/50 mol ratio sample of $\text{NaNO}_3/\text{KNO}_3$. This sample was melted and solidified at a cooling rate of $1\text{ }^\circ\text{C/hr}$ in the stationary furnace. A circular cross section of the solid was ground. The Raman mapping was based on 40×40 spectra providing the intensity ratio for the NaNO_3 and KNO_3 bands seen at ~ 1068 and $\sim 1050\text{ cm}^{-1}$. Spectral curves obtained in the light area (spectrum in blue, mostly NaNO_3) and in the dark blue area (spectrum in brown, mostly KNO_3) are given in Fig. 2B. Experimental: Pixel size and spatial resolution $1\text{ }\mu\text{m}$, 100 X objective, $180\text{ }\mu\text{m}$ confocal hole, $100\text{ }\mu\text{m}$ slit width, excited with 200 mW of 514.5 nm light, exposed twice for 1 second and averaged, followed by automatic cosmic-ray spike-removal. Note: The Raman spectral abscissa is not calibrated.

Fig. 3. This Raman microscope mapping (Fig. 3A) of a 50/50 mol ratio sample of $\text{NaNO}_3/\text{KNO}_3$ shows a structure which was the closest approach to laminar found in this work. This sample was melted and solidified by pushing it out of the furnace at a rate of 5 mm/hour. The Raman mapping was based on 40×40 spectra. Bands at ~ 1068 and $\sim 1050\text{ cm}^{-1}$ are due to NaNO_3 and KNO_3 , respectively. Examples of spectra are shown in Fig. 3B (spectrum in blue, mostly NaNO_3 , in brown, mostly KNO_3). Experimental: As in Fig. 2. Note: The Raman spectral abscissa is not calibrated.

Fig. 4. Raman microscope mappings (Fig. 4A & 4B) of a $\text{NaNO}_2/\text{NaNO}_3/\text{KNO}_3$ molar ratio mixture of 49.8/6.9/44.2. Fig. 4A shows the $\text{NaNO}_3/\text{KNO}_3$ and Fig. 4B the $\text{NO}_2^-/\text{NO}_3^-$ ratios obtained from the same set of 40×40 spectra. Typical Raman spectra are given in Fig. 4C, showing, from top to bottom, high (purple), low (brown) $\text{NaNO}_3/\text{KNO}_3$ mol ratios (ranges $1063\text{-}1078\text{ cm}^{-1}$ / $1046\text{-}1060\text{ cm}^{-1}$, white or dark on Fig. 4A) and high (blue), low (green) $\text{NO}_2^-/\text{NO}_3^-$ mol ratios (ranges $1315\text{-}1348\text{ cm}^{-1}$ / $1037\text{-}1079\text{ cm}^{-1}$, white or dark on Fig. 4B). The sample was melted and solidified by pushing at a rate of (5 mm/hour) out of the furnace. The solid was ground in paraffin and washed with n-pentane. Bands at ~ 1055 , ~ 1068 and $\sim 1329\text{ cm}^{-1}$ are due to KNO_3 , NaNO_3 and $(\text{Na/K})\text{NO}_2$, respectively. Experimental details: Pixel size and spatial resolution $1\text{ }\mu\text{m}$, 100 X objective, $180\text{ }\mu\text{m}$ confocal hole, $100\text{ }\mu\text{m}$ slit width, excited twice for 1 second with 200 mW of 514.5 nm light and averaged after spike-removal. Note: The Raman spectral abscissa is not calibrated.

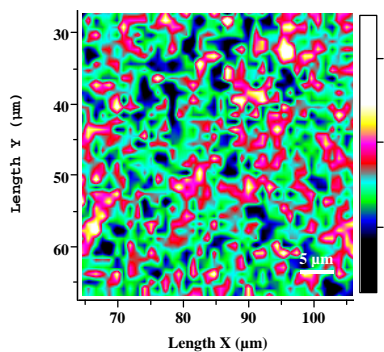


Fig. 1A

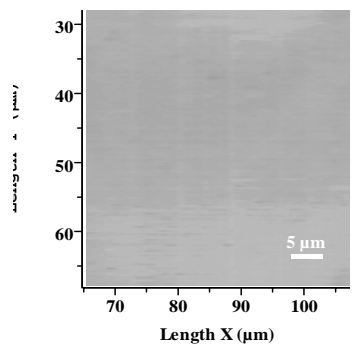


Fig. 1B

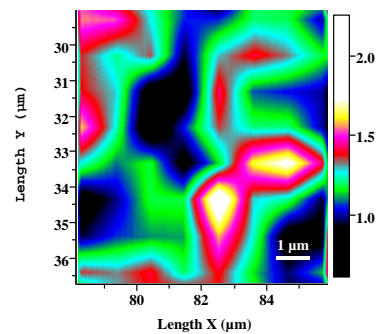


Fig. 1C

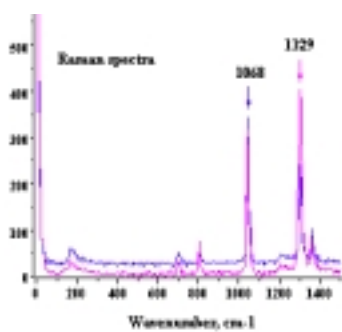


Fig. 1D

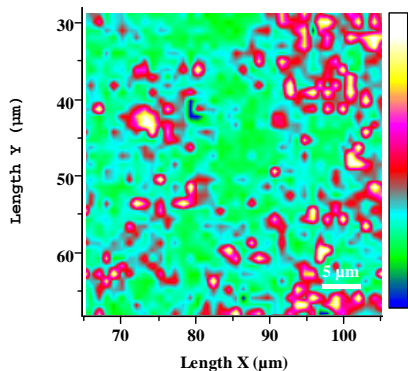


Fig. 2A

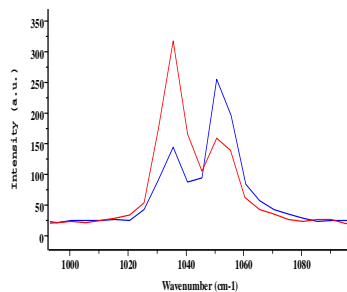


Fig. 2B

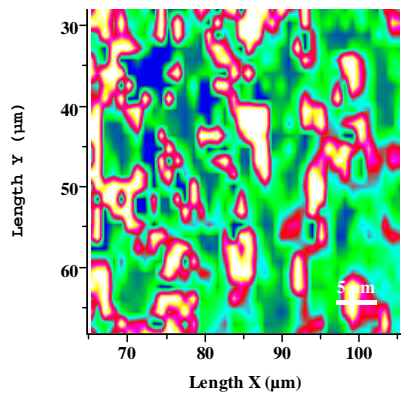


Fig. 3A

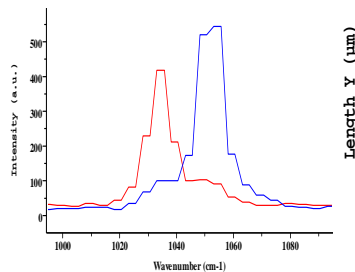


Fig. 3B

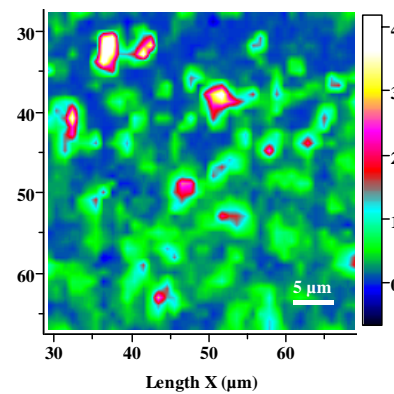


Fig. 4A

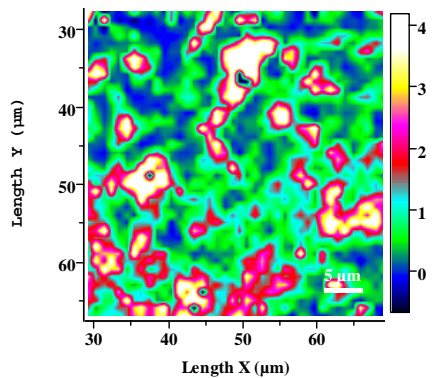


Fig. 4B

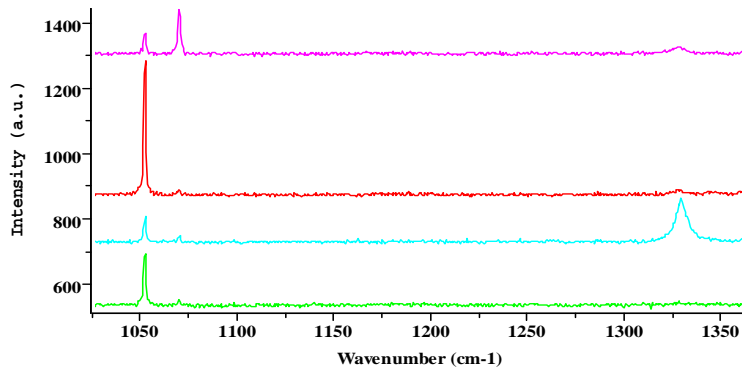


Fig. 4C

DISCUSSION

It is now clear that "conglomerate" structures are common, if not universal, for such comparatively low melting salt eutectics as those examined here. Certainly very large areas of interfacial contact between the constituent phases are indicated for all the systems studied, which is in accord with the deductions made from the solid electrical conductivity [6,7] and melting enthalpy measurements [8,9] made earlier, which indicated a structural enthalpy term of perhaps 55 J/g.

The question arises as to why the "conglomerate" structures found here, together with the observed diffuse crystallisation fronts (in the adapted zone refining furnace), should be so different from the lamellar and fibrous structures found by Hellowell et al. [1,2] and Trnovcova et al. [3,4] which require a linear crystallisation front. The answer seems to be that a linear front requires very good heat removal. Metals of course have thermal conductivities approximately two or more orders of magnitude greater than salts and hence lamellar structures would be expected to be more common. In addition it is significant that both the above groups of workers selected fluoride eutectics which have high melting points and thus would have much greater thermal gradients when being cooled by ambient air.

It must also be noted that Loxham and Hellowell [1] began their paper by considering all the phase diagrams formed by binary combinations of the alkali metal halides, but only chose to examine the structures of two salt eutectics, both fluorides, and both with the highest melting points. A further reason for choosing LiF as one component in these eutectics might have been its extremely low solubility in water and other solvents, and thus structures containing it can be more easily differentially etched. In a companion paper Hellowell et al. [2] devote considerable space to describing the difficulties of obtaining lamellae and showed that "irregular" structures were frequently obtained in the early stage of crystallisation, even when conditions were such that these latter later gave way to laminar structures. These remarks appear to refer to the metallic eutectics with which this paper [2] is chiefly concerned, but the problems appear general enough to be applicable to salt systems as well, and even more applicable when it is considered that the lower thermal conductivities impose lower thermal gradients with their inherent greater problems in maintaining linear crystallisation fronts. Difficulties which are further enhanced when using low melting salt eutectics.

Though the above discussion indicates that lamellar structures need not be expected generally for lower melting salt eutectics, it conversely indicates that "conglomerate" structures should be generally found. These are here shown by Raman microscopy to have such large areas of contact between the solid phases that the, so far universal finding of high electrical conductivities is explained. Also the presence of a "conglomerate" structure might be responsible for the difference of the melting enthalpies observed in many systems [8,9]. Furthermore the occurrence of "conglomerate" structures seems not to be dependant on the particular crystallisation conditions, as are lamellar and fibrous structures, and thus may be generally expected with samples of solidified salt eutectics.

Acknowledgements

Grateful thanks are expressed to the Danish Technical Science Research Foundation, the Corrit Foundation, the Tuborg Foundation, Danfoss A/S, Thomas B. Thrige Foundation, P. A. Fiskers Foundation and Direktor Ib Henriksen's Foundation for grants which made possible the purchase the DILOR Raman instrument and the LINKAM accessory; also to STVF for a travel grant to DHK and hospitality from DTU. The authors wish to thank Andy Horsewell of this University for helpful discussions.

REFERENCES

- [1] J. G. Loxham and A. Hellawell: *J. Amer. Ceram. Soc.*, Vol. **47** (1964), 184.
- [2] D. J. S. Cooksey, D. Munson, M. P. Wilkinson and A. Hellawell: *Phil. Mag.*, Vol. **10** (1964) 745.
- [3] V. Trnovcova, P. P. Fedorov, V. Labas and M. Y. Starostin: *Solid State Ionics; Science and Technology*, B. V. R. Chowdari et al. Eds, World Scientific Publishing Co., 1998, pp. 325-334.
- [4] V. Trnovcova, P. P. Fedorov, C. Barta, V. Labas, V. A. Meleshina and B. P. Sobolev: *Solid State Ionics*, Vol. **119** (1999) 173.
- [5] V. Trnovcova, P. P. Fedorov, I. L. Buchinskaya, V. Smatko and F. Hanic: *Solid State Ionics*, Vol. **119** (1999) 181.
- [6] E. I. Eweka and D. H. Kerridge: *Phys. Lett. A*, Vol. **174** (1993) 441.
- [7] E. I. Eweka: Ph.D. thesis, University of Southampton, 1992.
- [8] M. Gaune-Escard and D. H. Kerridge: "Advances in Molten Salts", M. Gaune-Escard Ed., Begell House Inc., New York, (1999), ISBN-567000-142-4, p. 270. See also M. Gaune-Escard and D. H. Kerridge: *The structure of Salt Eutectics*, *High Temp. Material Processes*, Vol **3**. (1999) 443-451.
- [9] D. H. Kerridge: "The Structure of Salt Eutectics", *Proc. Internatl. G. Papa-theodorou Symp.*, S. Boghosian, V. Dracopoulos, C. G. Kontoyannis and G. A. Voyiatis, Eds., Patras, Greece, (1999), ISBN-960-7839-01-3, p. 89.
- [10] P. Colarusso, L. H. Kidder, I. W. Levin and E. N. Lewis: *Raman and Infrared Microspectroscopy*, In "Encyclopedia of Spectroscopy and Spectrometry", Editors J. C. Lindon et al., Academic Press, New York, Vol. **3**, (1999), pp.1945.
- [11] K. Nakamoto: "Infrared and Raman Spectra of Inorganic and Coordination Compounds", Wiley Interscience, New York, part A, section II, (1997).
- [12] D. E. Irish and M. H. Brooker, *Adv. Infrared and Raman Spectrosc.*, Vol. **2** (1976) 212.
- [13] M. H. Brooker, *Can. J. Chem.*, Vol. **55** (1977) 1242-1250.
- [14] M. H. Brooker, *J. Phys. Chem. Solids*, Vol. **39** (1978) 657-667.
- [15] K. Xu and Y. Chen, *J. Raman Spectrosc.*, Vol. **30** (1999) 173-179 & 441-448.
- [16] R. W. Berg and T. Nørbygaard, In preparation for *Appl. Spectrosc.*
- [17] N. J. Bjerrum, R. W. Berg, D. H. Kerridge and J. H. von Barner: *Anal. Chem.*, Vol. **34** (1995) 2129.

- [18] J. H. von Barner, J. H. Andersen and R. W. Berg: *J. Mol. Liquids*, Vol. **83** Vol. **83** (1999) 141.
- [19] A. R. Ubbelohde: "The Molten State of Matter, Melting and Crystal Structure", Wiley & Sons, Chichester, UK., 1978.
- [20] P. A. Afanasiev, private communication.
- [21] A. Horsewell, private communication.
- [22] A. G. Bergman, S. I. Berul and I. N. Nikonova: *Izv. Sektora Fiz.-Khim. Analiza*, Vol. **23** (1953) 183.